ACS Photonics

Article

pubs.acs.org/journal/apchd5

Extreme and Quantized Magneto-optics with Graphene Meta-atoms and Metasurfaces

Yakir Hadad,*[,†,§] Artur R. Davoyan,*[,‡] Nader Engheta,*[,‡] and Ben Z. Steinberg*[,†]

[†]School of Electrical Engineering, Tel Aviv University, Ramat-Aviv, Tel-Aviv 69978, Israel

[‡]Department of Electrical and Systems Engineering, University of Pennsylvania, Philadelphia, Pennsylvania 19104, United States

Supporting Information

ABSTRACT: Graphene—a naturally occurring two-dimensional material with unique optical and electronic properties—serves as a platform for novel terahertz applications and miniaturized systems with new capabilities. Recent discoveries of unusual quantum magneto-transport and high magneto-optical activity in strong magnetic fields make graphene a potential candidate for nonreciprocal photonics. Here we propose a paradigm of a flatland graphene-based metasurface in which an extraordinary and quantized magneto-optical activity at terahertz and infrared is attained at low, on-chip-compatible, magnetizations (~0.2−0.3 T). The proposed system essentially breaks the tight linkage between the strength of the magnetic biasing and the resulting magneto-optical response. We design a system extremely sensitive to the quantized spectrum of graphene Landau levels and predict up to 90° of Faraday rotation with just a single sheet of graphene. We also demonstrate how to resolve the quantum resonances at the macroscopic level in the far-field. Our results not only are of a fundamental interest, but, as we discuss, pave a way to conceptually new capabilities in a range of applications, including sensing, terahertz nanophotonics, and even cryptography.

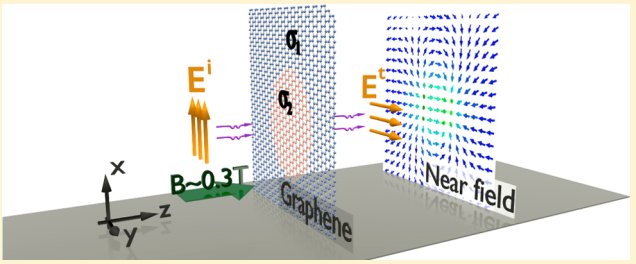

KEYWORDS: *nonreciprocity, graphene, Faraday effect, quasistatic resonators, optical nanodevices*

Graphene has attracted significant attention due to its gapless Dirac-type electron band gap structure and high electron mobility that allow for observing and exploiting novel regimes of classical and quantum electronic transport.[1−13] For instance, in an applied magnetic field electrons in graphene occupy a quantized set of energies, Landau levels,[14−23] giving rise to the quantum Hall effect. The latter is manifested not only in the peculiar electron transport in graphene but also in a high-frequency electromagnetic response of graphene. In particular, measurements of the electromagnetic wave transmission through single-layer and multilayer graphene in rather high magnetic fields (around 10 T) revealed a series of weak absorption resonances associated with transitions between different Landau levels.[24] Furthermore, rigorous study of the Faraday rotation in graphene demonstrated that graphene is a fascinating magneto-optical material: with just a single atomically thin layer, 6 degrees of polarization rotation at 7 T may be achieved in the lower terahertz frequency range (around 2−15 THz).[24,25] Fundamental limitations in the design of nonreciprocal graphene devices in certain configurations were given in ref 26.

The quantized spectrum of Landau-level-induced resonances and strong magneto-optical activity suggest graphene as a natural candidate for quantum and nonreciprocal photonics. However, a magnetically induced optical response in graphene, being pronounced at high magnetic field (several Teslas), implies a significant constraint for potential use and applicability of graphene. The magneto-optical activity drops significantly for low magnetic fields and high operating frequencies. For example, at 15 THz and 5 K and with a magnetic biasing of 7 T the Faraday rotation through a single graphene layer is about 0.5 deg; with biasing of 1 T the rotation is less than 0.1 deg.[24] Consequently, it is challenging to discern the Landau resonances, particularly at the upper terahertz range (>10 THz) and even in strong magnetic fields (~7 T).

Here we suggest a paradigm for graphene-based extreme nonreciprocal photonics and propose a concept of a graphene metasurface, in which an unprecedentedly strong magneto-optical activity (up to 90° of Faraday rotation) is attained at low magnetizations (even about 0.2−0.3 T) and thus enables the extreme enhancement of the quantum material properties. We design a graphene meta-atom and a metasurface that enhance the resolution of Landau-level resonances, implying a highly resolved, quantized spectrum of Faraday rotation.

RESULTS AND DISCUSSION

The electromagnetic response of a single graphene layer can be described by its complex conductivity ($\sigma = \sigma_r + i\sigma_i$), which depends on various parameters such as frequency ω, temperature T, charge carriers scattering rate Γ, chemical potential μ_c, and magnetic biasing field B; see, for example, the expressions

Received: July 29, 2014
Published: September 23, 2014

detailed in ref 22. Note that the imaginary part of the conductivity σ may be either positive or negative depending on the frequency and the local chemical potential. Therefore, a single graphene layer might serve as a platform for metamaterial engineering; by "patterning" the graphene sheet with different conductivity regions it may be possible to create one-atom-thick waveguides, cavities,[6,11] and more complicated systems.[10] Consider, for example, a suspended graphene sheet with conductivity σ_1 ($\mathrm{Im}\{\sigma_1\} < 0$), in which a circular region with conductivity σ_2 ($\mathrm{Im}\{\sigma_2\} > 0$) is induced, for example, by a local modulation of graphene's chemical potential; see Figure 1. This

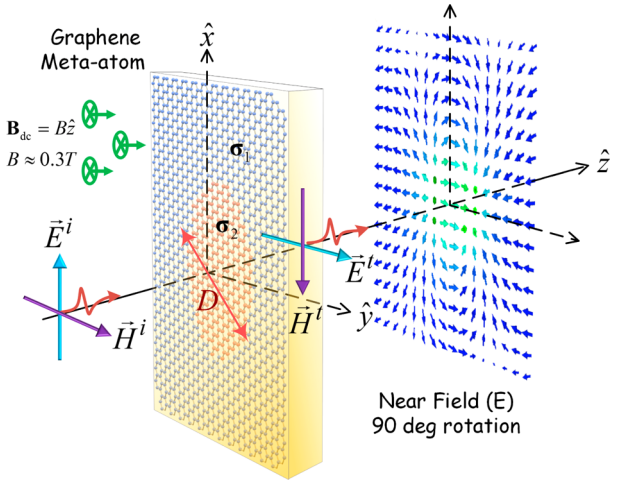

Figure 1. Schematic description of the concept. The "meta-atom" consists of a small circular region with a conductivity $\boldsymbol{\sigma}_2$ different from that in the rest of the graphene sheet ($\boldsymbol{\sigma}_1$), which is magnetized by a normal biasing magnetic field $\mathbf{B}_{dc}$. The grahene sheet is illuminated by an x-polarized electromagnetic plane wave. At resonance, an unprecedented 90° Faraday rotation of its electric field vector under a relatively weak biasing magnetic field of about 0.3 T in the near-zone occurs. The corresponding distribution of the electric field on a plane parallel with the graphene sheet at a distance of 1 nm is also shown.

circular region together with the rest of graphene may, under certain conditions, behave as a resonator analogous to an ultrathin metallic inclusion in an ultrathin dielectric slab, in which highly confined fields may be excited by an incident plane wave. In the limit of an infinitesimally small radius of the region with $\mathrm{Im}\{\sigma_2\} > 0$ the response of the system can be approximated quasistatically by a point dipole, which is resonantly excited when $\mathrm{Im}\{\sigma_1 + \sigma_2\}(\omega_r) = 0$ (more details in the Supporting Information). Within such a quasistatic (QS) limit, this resonance condition depends solely on the material properties, and hence the system becomes sensitive even to weak variations of graphene conductivity. As we show, such sensitivity leads to the dramatic enhancement of the intrinsic magneto-optical activity of graphene and hence enables the clear observation of otherwise weak material effects.

To illustrate this, we consider transmission of a normally incident x-polarized plane wave through a magnetized meta-atom in a Faraday geometry, as shown schematically in Figure 1. In this case the optical conductivity of the magnetically biased graphene is given by a conductivity tensor: $\sigma \rightarrow \boldsymbol{\sigma} = \sigma\mathbf{I} + ig\hat{z} \times \mathbf{I}$, where σ is the complex diagonal conductivity, g is the complex Hall conductivity responsible for the magneto-optical activity in graphene, e.g., for the Faraday rotation of the wave polarization, and $\mathbf{I}$ is the unit dyad. We find that in the proximity of our system, i.e., in the near-field, the Faraday rotation is given by (see the Supporting Information)

$$\theta_F = \arctan\left|\frac{E_{2,y}}{E_{2,x}}\right| = \arctan\left|\frac{g_1 - g_2}{\sigma_1 + \sigma_2}\right| \quad (1)$$

Clearly, at the resonance, i.e., when $\mathrm{Im}\{\sigma_1 + \sigma_2\}(\omega_r) = 0$, in the hypothetical lossless scenario, up to 90° Faraday rotation in the near-zone of the structure is possible, independent of the magnetic biasing, even if the latter is vanishingly small, as long as it is not identically zero. For a single graphene sheet this corresponds roughly to 3×10^5 deg/μm of polarization rotatio, a value far beyond any previous reports. In the realistic lossy scenario, at resonance $\mathrm{Im}\{\sigma_1 + \sigma_2\}(\omega_r) = 0$, the rotation angle θ_F depends on the quality factor (Q-factor) of the resonant meta-atom. At low temperatures and with a well-prepared graphene sample an unexpected, near 90°, polarization rotation is attainable, even with low magnetic bias, of 0.25−0.3 T. Note that a change of 0.06 eV (μ_{c1} = 0.1 eV, μ_{c2} = 0.16 eV) in the chemical potential is absolutely small, and although the relative difference is large (60%) in general, it will not greatly affect the material properties. However, in our case it yields a substantial difference between the characteristics of σ_1 and σ_2, as metal-like or dielectric-like, since we chose to work close to the border between the interband and intraband transition domains of graphene where the imaginary part of the conductivity changes its sign.

When sweeping the magnetic bias at fixed frequency, the meta-atom response is quantized and follows the Landau-level (LL) oscillations in the graphene; see Figure 2. At low magnetic bias the LL spectrum is dense and restrained; however our proposed meta-atom may enhance its resolution, opening the door for new possibilities to measure and utilize the dense LL spectrum at low magnetic bias. This dynamics is shown in Figure 2. Figure 2a shows the sum of imaginary parts of the diagonal conductivities $\mathrm{Im}\{\sigma_1 + \sigma_2\}$ for two cases. The first is for an ideal lossless system at T = 0 K, where the conductivities exhibit a quantized behavior with sharp LL transitions. The second is for a realistic low-loss scenario with ambient temperature T = 3 K and scattering coefficient Γ = 0.43 meV where the sharp transitions of $\mathrm{Im}\{\sigma_1 + \sigma_2\}$ are somewhat restrained. The corresponding quantized near-field Faraday polarization rotation is shown in Figure 2b. Above a low threshold $\mathbf{B}_{dc} > 0.25$ T, we observe a strong quantization of the polarization rotation versus magnetization. In particular two distinct states (0° and 90°) of polarization rotation exist even at low $\mathbf{B}_{dc}$ = 0.3−1 T. For a realistic system the angle of rotation, limited by the losses, exceeds 80° for $\mathbf{B}_{dc} > 0.4$ T. Interestingly, above this threshold, the maximally attainable Faraday rotation will not increase with an increase of the magnetic biasing, as opposed to any conventional magneto-optical system. The polarization rotation response follows the "chirped" shape of $\mathrm{Im}\{\sigma_1 + \sigma_2\}$ versus magnetization shown in Figure 2a. The quantized rotation of polarization is governed by the LL spectrum. The Faraday rotation angle through a pristine graphene (estimated by $\theta_F^{pr} \approx (180/\pi)\eta_0|g|$; see the Supporting Information) is much weaker than what may be obtained with our proposed meta-atom. Moreover the LL transition finesse in the pristine graphene is much more moderate and bias-field dependent (green line in Figure 2b). In contrast, the electrodynamic response of the proposed meta-atom is resonant and thus extremely sensitive also to weak changes in the material properties, e.g., by changing the magnetic bias.

dx.doi.org/10.1021/ph500278w | ACS Photonics 2014, 1, 1068−1073

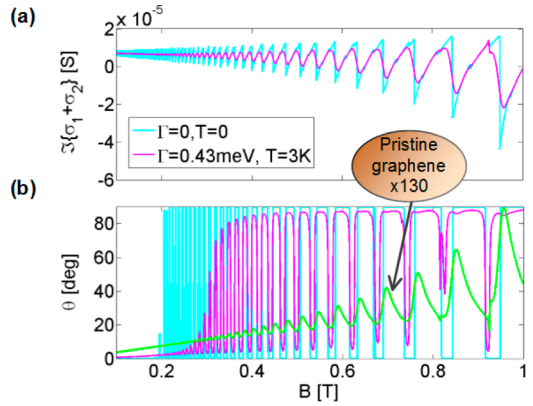

Figure 2. Optical conductivity and near-field Faraday rotation vs biasing magnetic field for a single inhomogeneous circular region on the graphene sheet (Figure 1). (a) The function $\mathrm{Im}\{\sigma_1 = \sigma_2\}(B)$ is depicted at fixed frequency 46.2 THz, for two cases: the hypothetical lossless material ($T = 0$ and $\Gamma = 0$) (pale blue) and the lossy material with $T = 3$ K and $\Gamma = 0.43$ meV (magenta). (b) Near-field Faraday rotation as obtained from eq 1. For comparison, the near-field Faraday rotation for the pristine graphene is also shown (green). For ease of comparison, the rotation for the pristine graphene is multiplied by 130 to be displayed in the same plot as the other Faraday rotations. The quasistatic resonance sharpens the field response and enhances the LL resolution and sensitivity by at least 2 orders of magnitude. The meta-atom response, quantized with the magnetic field, is clearly seen in the sharp $0° \rightarrow 90° \rightarrow 0°$ rotation transitions. In our simulations the region's diameter is taken to be $D = 8$ nm. The material conductivities are calculated by the Kubo formula[22] with the following parameters: chemical potentials outside and inside the region are $\mu_{c_1} = 0.1$ eV and $\mu_{c_2} = 0.16$ eV, the temperature is $T = 3$ K, and the scattering coefficient is $\Gamma = 0.43$ meV. The magnetic bias is assumed to be $\mathbf{B}_{dc} = 0.3$ T, directed normal to the graphene sheet.

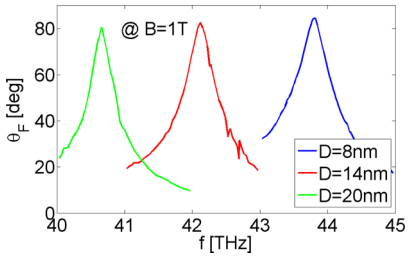

Figure 3. Resonance and strong rotation response as a function of frequency with different meta-atom diameters. Simulation carried out by CST Studio Suite. Magnetic bias $B_{dc} = 1$ T, lossy material with $T = 3k$ and $\Gamma = 0.43$ meV and chemical potentials $\mu_{c1} = 0.1$ eV and $\mu_{c2} = 0.16$ eV. As D grows, the resonance frequency is red-shifted with respect to the frequency obtained by the static approximation $f = 46.2$ THz (see Supporting Figure 2), but the rotation rate is very close to the analytic predication shown in Figure 2.

This makes our meta-atom an excellent sensor for the very weak LL transitions in graphene at low magnetic bias, as well as a very low magnetic bias polarization rotator. The latter is in fact an extraordinary enhancement of the Faraday rotation effect that results directly from the QS resonance. Recall that we work in the QS regime, and therefore formally $D \ll \lambda_{spp}$ (λ_{spp} is the smallest wavelength in the problem). Nevertheless, high-order off-resonance multipoles are negligible when the dipolar resonance condition is satisfied. Therefore, as D grows (but still $\lesssim\lambda_{spp}$), the QS dipolar resonance and the strong rotation effects remain but are red-shifted. This is shown in Figure 3 with $D = 8$, 14, and 20 nm. Note that with $D = 20$ nm our classical model is strictly valid, and the extreme enhancement of the Faraday effect, achieving nearly 90° rotation with magnetization of about 1 T at above 40 THz, still exists. However, with smaller D, quantum effects discussed in ref 27 may shift and somewhat weaken the QS resonance.

Such a quantum meta-atom can serve as a platform for more complicated structures. However, the results shown in Figure 2b pertain only to the near-field of a single meta-atom and are, in principle, challenging to measure. Far-field measurement of Faraday rotation is far more common, but unfortunately the response of a single meta-atom cannot be directly observed in the far zone since the incident field diffracts around the meta-atom and overwhelms its response. To overcome this difficulty, here, as an example, we develop principles of a quantum magneto-active metasurface for which we suggest a metasurface that consists of an appropriately patterned periodic lattice of the proposed meta-atom. This one-atom-thick metasurface can expose the enhancement properties of our meta-atom, also in the far zone. The high sensitivity of a single meta-atom and its strong near-field Faraday response are projected to the macroscale metasurface and to its far-field response (see Supporting Information). Such a response is essentially the averaged response of the near-field and, thus, depends on the unit-cell filling factor (defined as the ratio between the meta-atom area and the lattice unit-cell area). To optimize the latter, we use a hexagonal lattice as shown in Figure 4a. Its unit cell parameters are diameter $D = 8$ nm and lattice constant $a = 12$ nm. Other graphene parameters are as before. With this configuration we obtain about 18° rotation in the far-field with about 0.3 T magnetic bias at about 45 THz. Sharp quantized transitions of the polarization angle are clearly observed in this case as well (Figure 4b). We note that the Faraday rotation in a pristine graphene with $\mathbf{B}_{dc} = 0.3$ T at 45 THz is less than 0.1°; that is, with the suggested metasurface we obtain more than 2 orders of magnitude enhancement in the Faraday rotation. This fact suggests the great possibility of performing measurements of the LL spectrum with very weak magnetic bias, in the far-field of the sample. Note that due to the finite size of the meta-atom region, the resonance frequency experiences a small red-shift compared to the QS solution.[10]

Note that the circular region of the meta-atom in the metasurface in the presence of magnetic bias has a different response to the left- and right-handed circularly polarized light. In particular, the absorption of these circular polarizations differs significantly, resulting in a huge circular dichroism though a monolayer of atoms. In Figure 4c the circular dichroism is plotted versus magnetization. We note that the definition of circular dichroism in our case is somewhat subtle, and a detailed discussion is given in the Supporting Information.

The proposed meta-atom is a highly sensitive, controllable, and tunable unit cell that can be used in the design of a variety of novel magneto-optical components with exciting properties. It opens new possibilities for low-magnetic-bias LL spectrum measurements and Faraday rotation in both near-field and far-field. Since it strongly responds to the magnetization bias even when the bias is weak, the proposed quantum metastructure has a promising potential in making magneto-optical effects on-chip usable, e.g., as ultrathin polarization rotators; due to the large rotation achievable with a single layer, one may need only a single graphene layer or a stack of only a small number of layers (between 2 and 4) to achieve any rotation between 0° and 90°

dx.doi.org/10.1021/ph500278w | ACS Photonics 2014, 1, 1068−1073

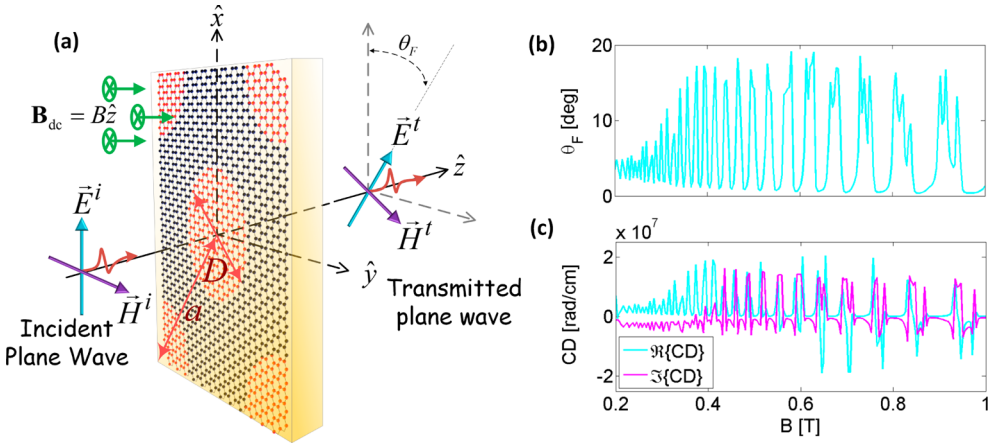

Figure 4. Far-field Faraday rotation and circular dichroism for a hexagonal periodic array of the inhomogeneous circular regions on the graphene sheet. (a) Geometry of a single unit cell of the periodic hexagonal array. The diameter of circular region is D = 8 nm and lattice constant a = 12 nm. Simulation results for (b) far-field Faraday rotation and (c) circular dichroism (real (pale blue), imaginary (magenta)), vs biasing magnetic field at a fixed frequency of 42.7 THz. Other parameters are as above.

(see Figure 5). In this case, after N layers the transmission is given by $T_N = T^N$, whereas the rotation by $\theta_N = N\theta_F$ where T and θ_F are the transmission and rotation through a single layer. Note that in order to enhance transmission through the stack, the usage of an asymmetric array unit cell may be desirable as discussed in the Supporting Information. Our meta-atom can also be used as a switch, or as a building block of a highly nonreciprocal *completely planar* optical one-way guiding chain of nanoscale transverse dimensions akin to the one suggested and studied in refs 28 and 29. Moreover, the proposed meta-atom can be used for encryption at the nanoscale as illustrated in Figure 6. For example, the two orthogonal near-field polarizations of a meta-atom can be referred to as binary digits, say, "$\hat{x}$" for "0" and "$\hat{y}$" for "1". Then, due to the high sensitivity of the near-field polarization to the magnetic biasing around resonance and due to the different magnetic-biasing locations at which the LL transitions take place for different frequencies, arrays of meta-atoms at slightly different chemical potentials, shapes, or sizes can be used to encrypt a barcode. Once encoded, the barcode can be read correctly using a near-field scanner and only by an agent who has a preknowledge of the exact magnetic biasing and resonance frequency at which it was

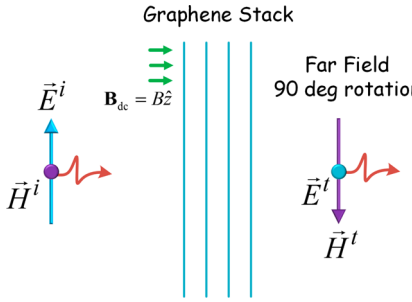

Figure 5. Graphene stack. The number of layers is fixed according to the required rotation after the stack. The spacing between the layers should be on the order of or larger than the typical unit-cell size. Therefore, using our scheme of electrically small unit cells the total stack thickness can be very small.

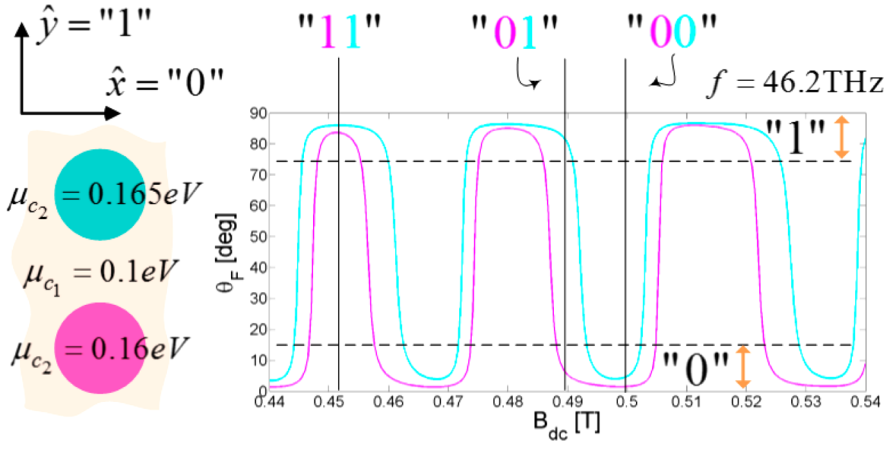

Figure 6. Barcode encryption with an array of several meta-atoms. In this example two meta-atoms with identical parameters except for their chemical potential μ_{c_2} are surrounded by graphene with μ_{c_1} = 0.1 eV. The excitation response is shown at the fixed frequency 46.2 THz as a function of the magnetic biasing. The sharp transitions make it possible to treat the polarization rotation signal as a digital signal. We chose to define the polarization close to x (y) as binary "0" ("1"). When read, the binary word depends on the specific combination of optical frequency and magnetic biasing. Thus, this configuration can be used for encryption.

dx.doi.org/10.1021/ph500278w | ACS Photonics 2014, 1, 1068−1073

encoded. Last but not least, due to the extremely large slope at the LL transitions (see red line in Figure 2b), a single meta-atom with biasing of about 0.2−0.3 T with a precise value near an LL transition will exhibit a significant change in rotation of an incident electric field even under very small changes of the ambient magnetic field. Hence, it can be used as a highly sensitive sensor for weak magnetic fields with applications in, for example, magnetic memory reading or ultralow magnetic field sensing.

As a final remark, note that patterns of chemical potential can be obtained by electric gating,[6,11] plasmon-induced doping,[30] or chemical doping.[31−33] Due to the fringing fields between the electrode and the graphene layer, electrical gating will yield a conductivity transition region that we believe will essentially shift the resonance.[11] This transition can be sharpened by bringing the electrode and the graphene layer close together; however in this case the mutual interaction should be taken into account. Chemical doping, however, has been achieved experimentally down to the level of a single molecule or even a single atom and therefore may be used to create sharply defined chemical potential regions.

METHODS

This work is theoretical. The analysis that leads to our results, e.g., in eq 1 and the data provided in the figures, is based on a mathematical derivation of the meta-atom response by using the Kubo formula for the graphene surface impedance. The electromagnetic response is derived with this impedance under the assumption of QS excitation (i.e., the circular region of different conductivity is much smaller than the wavelength). The analytical results were then verified using full-wave numerical simulation. More details are provided in the Supporting Information.

CONCLUSIONS

A novel paradigm for a significant enhancement of the Faraday effect in thin magneto-optical materials was proposed. The method suggests replacing the requirement for high magnetic biasing by a different requirement for low loss. In the limiting case of lossless material it was shown that the relation between the magneto-optical activity of the material and the magneto-optical response is essentially decoupled, yielding a possibility to have 90° Faraday rotation with vanishingly small magnetic biasing. Furthermore, note that although this work was concerned with graphene the general idea is valid for any system that can be modeled as a two-dimensional free electron gas, such as thin layers of doped semiconductors, etc. Therefore, the mechanism introduced by this work opens new venues for theoretical as well as experimental research in the field and has a potential to contribute in real on-chip implementations.

ASSOCIATED CONTENT

Supporting Information

The Supporting Information includes detailed zero- and first-order QS calculation of the system response and investigation of its characteristics, analytic study of the array problem, and detailed explanation of the numerical simulations. This material is available free of charge via the Internet at http://pubs.acs.org.

AUTHOR INFORMATION

Corresponding Authors

*E-mail: yakhadad@gmail.com.
*E-mail: davoyan@seas.upenn.edu.
*E-mail: engheta@ee.upenn.edu.
*E-mail: steinber@eng.tau.ac.il.

Present Address

§Department of Electrical and Computer Engineering, The University of Texas at Austin, 1 University Street C0803, Austin, Texas 78712, United States.

Notes

The authors declare no competing financial interest.

ACKNOWLEDGMENTS

Y.H. and B.Z.S. acknowledge support from the Israeli Science Foundation (Grant 1503/10). A.R.D. and N.E. acknowledge support from the U.S. Air Force Office of Scientific Research (AFOSR) Multidisciplinary University Research Initiative (MURI) on Quantum Metamaterials and Quantum Metaphotonics, Grant No. FA 9550-12-1-0488.

REFERENCES

(1) Novoselov, K. S.; Geim, A. K.; Morozov, S. V.; Jiang, D.; Katsnelson, M. I.; Grigorieva, I. V.; Dubonos, S. V.; Firsov, A. A. Two-Dimensional Gas of Massless Dirac Fermions in Graphene. *Nature* **2005**, *438*, 197−200.

(2) Geim, A. K.; Novoselov, K. S. The Rise of Graphene. *Nat. Mater.* **2007**, *6*, 183−191.

(3) Li, Z. Q.; Henriksen, E. A.; Jiang, Z.; Hao, Z.; Martin, M. C.; Kim, P.; Stormer, H. L.; Basov, D. N. Dirac Charge Dynamics in Graphene by Infrared Spectroscopy. *Nat. Phys.* **2008**, *4*, 532−535.

(4) Yan, H.; Li, X.; Chandra, B.; Tulevski, G.; Wu, Y.; Freitag, M.; Zhu, W.; Avouris, P.; Xia, F. Tunable Infrared Plasmonic Devices Using Graphene/Insulator Stacks. *Nat. Nanotechnol.* **2012**, *7*, 330−334.

(5) Davoyan, A. R.; Popov, V. V.; Nikitov, S. A. Tailoring Terahertz Near-Field Enhancement via Two-Dimensional Plasmons. *Phys. Rev. Lett.* **2012**, *108*, 127401.

(6) Vakil, A.; Engheta, N. Transformation Optics Using Graphene. *Science* **2011**, *332*, 1291−1294.

(7) Padooru, Y. R.; Yakovlev, A. B.; Kaipa, C. S. R.; Hanson, G. W.; Medina, F.; Mesa, F. Dual Capacitive-Inductive Nature of Periodic Graphene Patches: Transmission Characteristics at Low-Terahertz Frequencies. *Phys. Rev. B* **2013**, *87*, 115401.

(8) Christensen, J.; Manjavacas, A.; Thongrattanasiri, S.; Koppens, F. H. L.; de Abajo, F. J. G. Graphene Plasmon Waveguiding and Hybridization in Individual and Paired Nanoribbons. *ACS Nano* **2012**, *6*, 431−440.

(9) Koppens, F. H. L.; Chang, D. E.; Abajo, F. J. G. De. Graphene Plasmonics: A Platform for Strong Light−Matter Interactions. *Nano Lett.* **2011**, 3370−3377.

(10) Hadad, Y.; Steinberg, B. Z. Quasistatic Resonance of a Chemical Potential Interruption in a Graphene Layer and Its Polarizability: The Mixed-Polarity Semilocalized Plasmon. *Phys. Rev. B* **2013**, *88*, 075439.

(11) Forati, E.; Hanson, G. W. Surface Plasmon Polaritons on Soft-Boundary Graphene Nanoribbons and Their Application in Switching/Demultiplexing. *Appl. Phys. Lett.* **2013**, *103*, 133104.

(12) Fallahi, A.; Perruisseau-Carrier, J. Design of Tunable Biperiodic Graphene Metasurfaces. *Phys. Rev. B* **2012**, *86*, 195408.

(13) Alonso-Gonzalez, P.; Nikitin, A. Y.; Golmar, F.; Centeno, A.; Pesquera, A.; Velez, S.; Chen, J.; Navickaite, G.; Koppens, F.; Zurutuza, A.; Casanova, F.; Hueso, L. E.; Hillenbrand, R. Controlling Graphene Plasmons with Resonant Metal Antennas and Spatial Conductivity Patterns. *Science* **2014**, 1369.

(14) Sadowski, M. L.; Martinez, G.; Potemski, M. Landau Level Spectroscopy of Ultrathin Graphite Layers. *Phys. Rev. Lett.* **2006**, *97*, 266405.
(15) Taychatanapat, T.; Watanabe, K.; Taniguchi, T.; Jarillo-Herrero, P. Quantum Hall Effect and Landau-Level Crossing of Dirac Fermions in Trilayer Graphene. *Nat. Phys.* **2011**, *7*, 621−625.
(16) Jiang, Z.; Henriksen, E. A.; Tung, L. C.; Wang, Y.-J.; Schwartz, M. E.; Han, M. Y.; Kim, P.; Stormer, H. L. Infrared Spectroscopy of Landau Levels of Graphene. *Phys. Rev. Lett.* **2007**, *98*, 197403.
(17) Park, C.-H.; Son, Y.-W.; Yang, L.; Cohen, M.; Louie, S. Landau Levels and Quantum Hall Effect in Graphene Superlattices. *Phys. Rev. Lett.* **2009**, *103*, 046808.
(18) Li, G.; Luican-Mayer, A.; Abanin, D.; Levitov, L.; Andrei, E. Y. Evolution of Landau Levels into Edge States in Graphene. *Nat. Commun.* **2013**, *4*, 1744.
(19) Zhang, Y.; Jiang, Z.; Small, J. P.; Purewal, M. S.; Tan, Y.-W.; Fazlollahi, M.; Chudow, J. D.; Jaszczak, J. A.; Stormer, H. L.; Kim, P. Landau-Level Splitting in Graphene in High Magnetic Fields. *Phys. Rev. Lett.* **2006**, *96*, 136806.
(20) Luican, A.; Li, G.; Andrei, E. Y. Quantized Landau Level Spectrum and Its Density Dependence in Graphene. *Phys. Rev. B* **2011**, *83*, 041405.
(21) Miller, D. L.; Kubista, K. D.; Rutter, G. M.; Ruan, M.; de Heer, W. A.; First, P. N.; Stroscio, J. A. Observing the Quantization of Zero Mass Carriers in Graphene. *Science* **2009**, *324*, 924−927.
(22) Gusynin, V. P.; Sharapov, S. G.; Carbotte, J. P. Magneto-Optical Conductivity in Graphene. *J. Phys.: Condens. Matter* **2007**, *19*, 026222.
(23) Bolotin, K. I.; Ghahari, F.; Shulman, M. D.; Stormer, H. L.; Kim, P. Observation of the Fractional Quantum Hall Effect in Graphene. *Nature* **2009**, *462*, 196−199.
(24) Crassee, I.; Levallois, J.; Walter, A. L.; Ostler, M.; Bostwick, A.; Rotenberg, E.; Seyller, T.; van der Marel, D.; Kuzmenko, A. B. Giant Faraday Rotation in Single- and Multilayer Graphene. *Nat. Phys.* **2010**, *7*, 48−51.
(25) Crassee, I.; Levallois, J.; van der Marel, D.; Walter, A. L.; Seyller, T.; Kuzmenko, A. B. Multicomponent Magneto-Optical Conductivity of Multilayer Graphene on SiC. *Phys. Rev. B* **2011**, *84*, 035103.
(26) Tamagnone, M.; Fallahi, A.; Mosig, J. R.; Perruisseau-carrier, J. Fundamental Limits and near-Optimal Design of Graphene Modulators and Non-Reciprocal Devices. *Nat. Photonics* **2014**, 1−13.
(27) Thongrattanasiri, S. Quantum Finite-Size Effects in Graphene Plasmons. *ACS Nano* **2012**, *6*, 1766−1775.
(28) Mazor, Y.; Steinberg, B. Z. Longitudinal Chirality, Enhanced Nonreciprocity, and Nanoscale Planar One-Way Plasmonic Guiding. *Phys. Rev. B* **2012**, *86*, 045120.
(29) Hadad, Y.; Mazor, Y.; Steinberg, B. Z. Green's Function Theory for One-Way Particle Chains. *Phys. Rev. B* **2013**, *87*, 035130.
(30) Fang, Z.; Wang, Y.; Liu, Z.; Schlather, A.; Ajayan, P. M.; Koppens, F. H. L.; Nordlander, P.; Halas, N. J. Plasmon-Induced Doping of Graphene. *ACS Nano* **2012**, *6*, 10222−10228.
(31) Natan, A.; Hersam, M. C.; Seideman, T. Insights into Graphene Functionalization by Single Atom Doping. *Nanotechnology* **2013**, *24*, 505715.
(32) Balog, R.; Jørgensen, B.; Nilsson, L.; Andersen, M.; Rienks, E.; Bianchi, M.; Fanetti, M.; Laegsgaard, E.; Baraldi, A.; Lizzit, S.; Sljivancanin, Z.; Besenbacher, F.; Hammer, B.; Pedersen, T. G.; Hofmann, P.; Hornekaer, L. Bandgap Opening in Graphene Induced by Patterned Hydrogen Adsorption. *Nat. Mater.* **2010**, *9*, 315−319.
(33) Coletti, C.; Riedl, C.; Lee, D. S.; Krauss, B.; Patthey, L.; von Klitzing, K.; Smet, J. H.; Starke, U. Charge Neutrality and Band-Gap Tuning of Epitaxial Graphene on SiC by Molecular Doping. *Phys. Rev. B* **2010**, *81*, 235401.